RELIABLY FLATTENED RADAR BACKSCATTER FOR WET SNOW MAPPING FROM WIDE-SWATH SENSORS

David Small [(1)], Nuno Miranda [(2)], Tracy Ewen [(3)], Tobias Jonas [(4)]

[(1)] Remote Sensing Laboratories (RSL), U of Zurich, Winterthurerstrasse 190; CH-8057 Zurich; Switzerland, Email: david.small@geo.uzh.ch

[(2)] European Space Agency ESRIN, Frascati, Italy, Email: nuno.miranda@esa.int

[(3)] Hydrology and Climate (H2K), U of Zurich, Winterthurerstrasse 190; CH-8057 Zurich; Switzerland, Email: tracy.ewen@geo.uzh.ch

[(4)] WSL Institute for Snow and Avalanche Research SLF, Flüelastrasse 11; CH-7260 Davos; Switzerland, Email: tobias.jonas@slf.ch

ABSTRACT

Retrieval of wet snow extent with high temporal resolution over large areas that include topography requires use of wide swath SAR and radiometric terrain correction to enable backscatter comparisons across different orbital tracks. We report on springtime wet snow mapping using a time series of Envisat ASAR wide swath (WS) images covering the Swiss Alps. The ASAR observations were used to constrain a runoff model for a local catchment; performance was assessed with and without integration of the radar data. Our EOPI project began an unprecedentedly dense series of ASAR WS acquisitions over Switzerland in March 2012. Wet snow maps at the *national* scale were generated and integrated for the first time on an *operational* basis within the Swiss Institute for Snow and Avalanche Research SLF. Lessons learned from this initial operational integration test are discussed, with a view toward the monitoring possibilities coming soon with the Sentinel-1 radar satellites.

1 INTRODUCTION

Modern SAR sensors offer wide swath modes that enable generally more frequent revisit times to monitor large regions. For example, the Envisat ASAR sensor was able to acquire imagery in either relatively high *spatial* resolution (Image Mode) with a 100km swath width, or higher *temporal* resolution (Wide Swath Mode) with a 400km swath width [12].

Early attempts to retrieve snow covered area (SCA) or alternatively wet snow extent (SE) focussed on data from the ERS-1 and ERS-2 satellites with their 100km swath [3]. The strongest dynamic was observed in wet snow conditions during the springtime melt season [8]. Multitemporal ratios (or dB-differences) were soon found to be an effective way of identifying wet snow signatures [13][16]. Given an exact-repeat interval, multitemporal ratios work also in mountainous regions [25]. Initial work with wider swath ScanSAR imagery from the Radarsat-1 satellite concentrated on relatively flat forest areas [9] or exact orbit repeat intervals [7][11]. The typical ERS mission repeat-orbit interval of 35 days and the narrow swath combined to limit the achievable temporal revisit anywhere outside the extremely high latitudes. That situation continued with Envisat ASAR sensor's 35-day orbit and most-common 100km swath ERS-compatible image mode (IM) beam IS2 acquisition pattern. Relaxation of the exact orbit repeat requirement becomes possible when terrain-induced backscatter variations are first flattened, creating a "level playing field" for comparisons across orbital tracks. Although this is a central issue when monitoring snow in mountainous regions, it is often not discussed, e.g. a recent review of seasonal snow monitoring methodologies [14] made no mention of the effects of terrain on SAR-based wet snow retrievals.

To improve the frequency of available observations, we proposed to ESA in the frame of EOPI project 10331 that IM acquisitions should be limited as far as possible in the Swiss Alpine springtime melt period of 2012, in favour of the wide swath (WS) mode. The proposal was approved by ESA. The springtime melt period in the Swiss Alps typically runs from the beginning of March until the end of June. From the end of Feb. 2012 until April 7th, Envisat acquired images of Switzerland with an unprecedented revisit interval. Sadly, just as the melt season was beginning in earnest, contact with the satellite was lost on April 8, and the remainder of the planned dataset could not be acquired [12]. In this paper, we describe analyses we performed on the set of 2012 data that was acquired as well as archival datasets.

2 ASAR WIDE SWATH PROCESSING

Although simple ratios or dB-differences with respect to a dry winter reference image suffice given an exact repeat, in mountainous regions, if one wishes to have temporal revisit at a rate faster than the exact repeat (35 days for Envisat), then radiometric terrain correction is mandatory. Many tried using the local incident *angle* as a proxy for the local *area* seen by the radar, deriving a correction factor from the local slope angle [6] calculated using a digital elevation model (DEM).

Proc. 'ESA Living Planet Symposium 2013', Edinburgh, UK 9–13 September 2013 (ESA SP-722, December 2013)

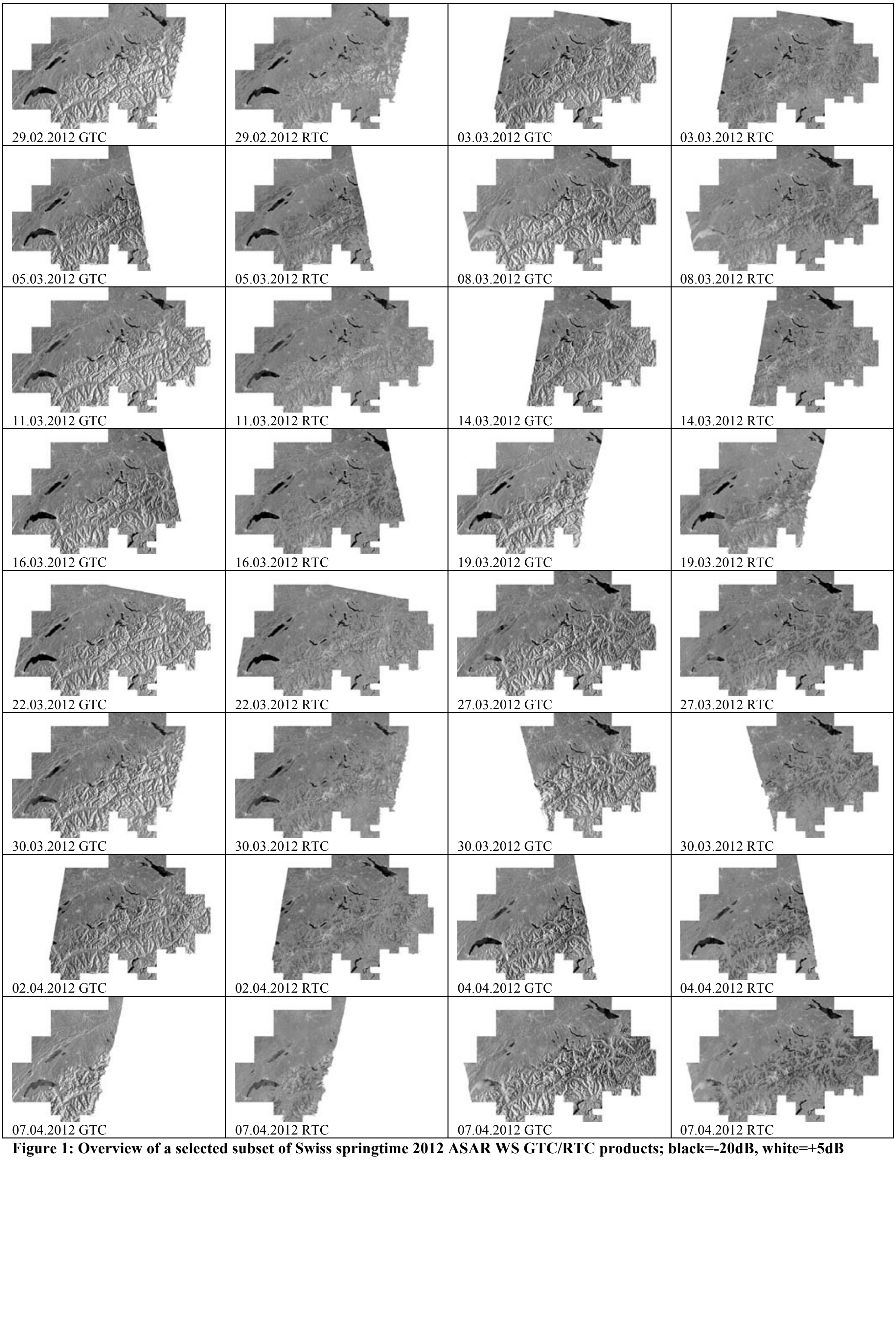

Figure 1: Overview of a selected subset of Swiss springtime 2012 ASAR WS GTC/RTC products; black=-20dB, white=+5dB

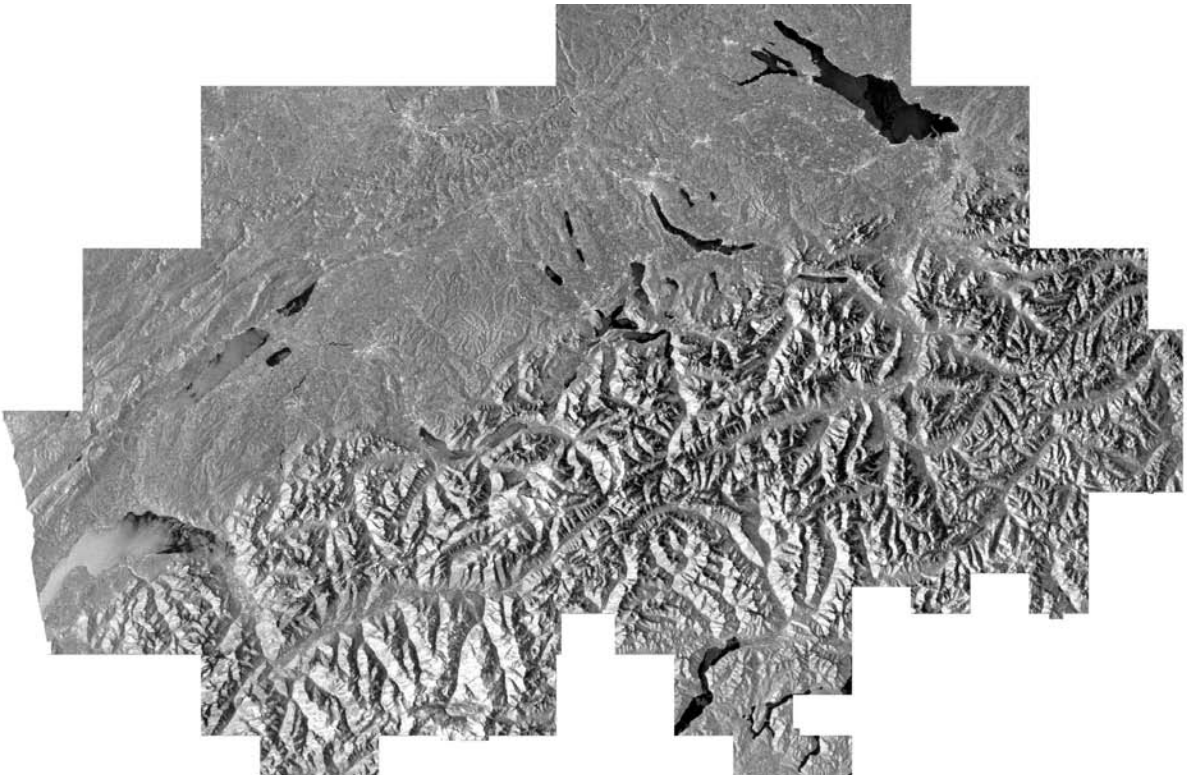

(a) Geometrically Terrain Corrected γ_E^0 (GTC) Backscatter – ASAR WS 07-APR-2012 – swisstopo DHM25 used

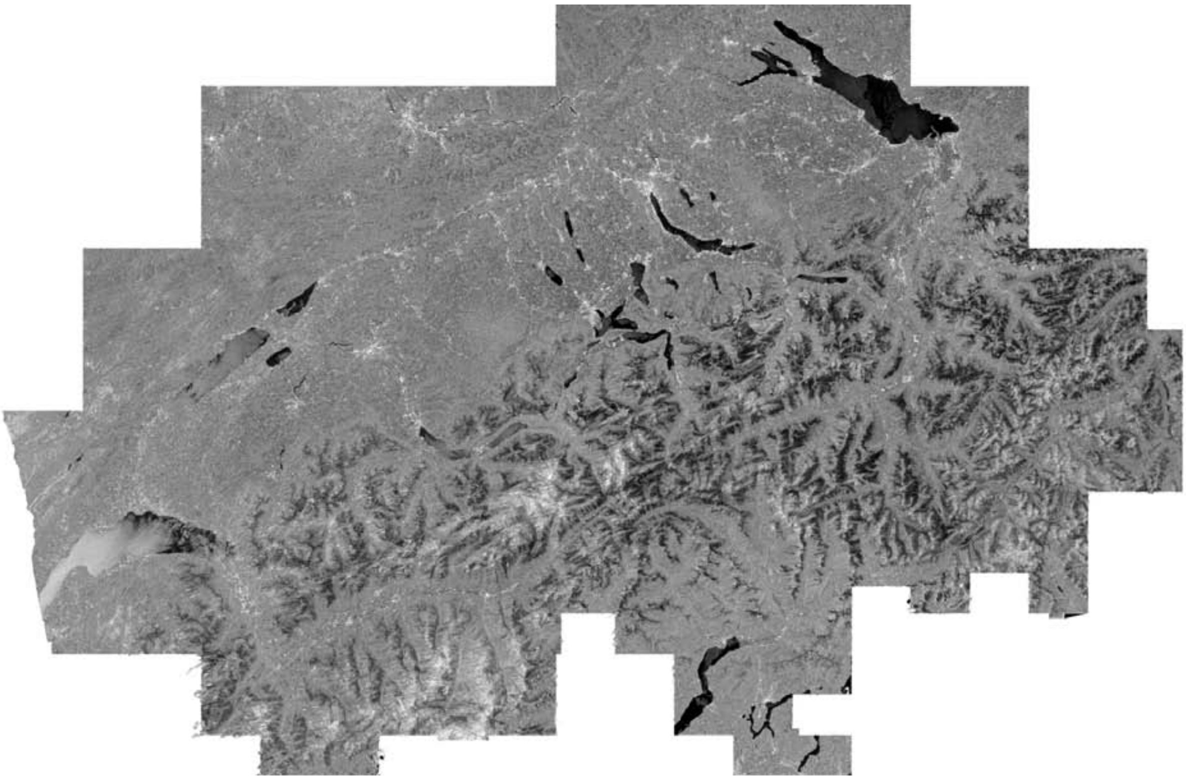

(b) Radiometrically Terrain Corrected γ_T^0 (RTC) Backscatter – ASAR WS 07-APR-2012 – swisstopo DHM25 used

Figure 2: ASAR Wide Swath (WS) VV-polarisation 07-APR-2012 Backscatter (a) Ellipsoid-flattened (GTC), (b) Terrain-flattened Gamma Nought (RTC) of Switzerland from the day before contact was lost with Envisat; black=-20dB, white=+5dB

2.1 Radiometric terrain correction (RTC)

In recent years, a highly refined radiometric image simulation methodology has been developed at RSL, U of Zurich. It follows the gamma nought radar backscatter convention, whereby the relevant contributing area on the ground "seen" by the radar is taken to be the component visible in the plane perpendicular to the radar look direction [23]. The method iterates through a DEM, adding up all non-shadowed contributions from terrain-facets *visible to the radar* and in the process builds up a reference image "simulation" [22]. The simulation output product is a measure of the local area contributing to the observation at each range and azimuth coordinate in the image and was shown to provide superior correction to angle-derived proxies [22]. The method is generally applicable to SAR data, and has been demonstrated using ASAR, PALSAR [2], and Radarsat-2 data [21].

2.2 Time Series

Beginning at the end of Feb. 2012, the EOPI project 10331 began an unprecedentedly dense series of ASAR WS acquisitions over Switzerland. A dense time series enables optimal application of a combination of RTC and backscatter compositing techniques [20]. From March to April 2012, ASAR WS products were downloaded from ESA and processed to the RTC level within a day. The orbital state vectors used were those included in the product, typically AUX_FRO (*restituted*), or occasionally AUX_FPO (*predicted*). There were exceptional cases where an old *predicted* quality state vector set was included in the product, and this negatively impacted the quality of the resulting RTC products. However, within 3 days, the DORIS *preliminary* orbit products were always available: these were used to regenerate RTC images for the complete dataset with a separate 3-day lag. A representative subset of the time series of GTC and RTC images is shown in Figure 1. The last image in the series, acquired on the day before contact was lost with Envisat, is shown with greater detail in Figure 2. Note how thematic land-cover (e.g. snow melting) is mixed together with the backscatter induced by topographic variations in the GTC product shown in (a). Most of the topographic component is corrected in the RTC product shown in (b). N.B.: both images are derived from the same data acquisition and all processing is automatic: no tiepoint-based refinement is necessary from modern SAR sensors with high quality state vectors and well-calibrated radar timing annotations [18].

It was planned to use the RTC time series as the basis for two studies: (a) a catchment analysis in northeastern Switzerland, and (b) operational integration at the national scale for snow hydrology modeling. The shortened 2012 dataset was too brief for the planned catchment study, so archival data acquired with longer less optimal revisit intervals were substituted. The 2012 dataset was used for operational integration testing as well as a supplement to earlier studies based on archival ASAR WS acquisitions from 2002 to 2011.

3 CATCHMENT STUDY

Information based on ASAR-based wet snow maps for the period 2007-2010 was used to better constrain runoff generation for the *Rietholzbach* catchment, an unmanaged alpine catchment in Switzerland, using the conceptual rainfall-runoff model, HBV, developed in Sweden [4]. The HBV model set-up used for this study employs a multivariate calibration technique and updates the snowmelt routine with water content estimates derived from the wet snow maps. Although recent studies have shown improved runoff prediction with incorporation of satellite snow cover information into the calibration of hydrological models (e.g. [1][15]), no study to our knowledge has directly incorporated snowmelt information in this way.

3.1 Method

The percentage of wet snow in the catchment is derived from the wet snow maps by calculating the difference between a wet snow image and a dry reference image, with a threshold to detect wet snow [13]. At each time step where a snow map is available, the percentage of wet snow calculated from the wet snow maps (Figure 3) is then used directly as input to HBV as water content for the snow routine (Figure 5). The HBV model uses precipitation and temperature as input at a daily time-step, and monthly mean evaporation. Daily runoff is used to calibrate the model with a multivariate calibration technique using a Genetic Algorithm and Powell optimization (GAP) [19].

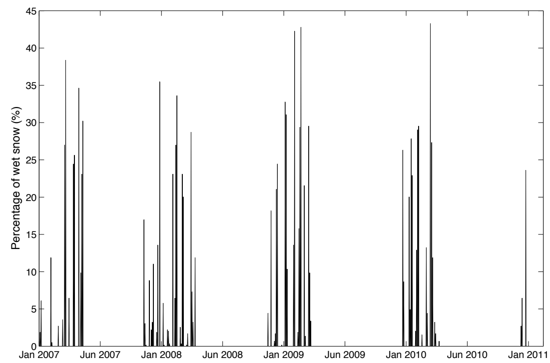

Figure 3: Percentage of wet snow, from wet snow maps

3.2 Results

Model performance was assessed based on observed versus simulated runoff with and without an update of water content derived from the wet snow maps (simulations with and without ASAR). Figure 4 shows observed and simulated model runoff for both simulations. Improvements can be seen for some events with higher flow observed in simulations incorporating ASAR observations, e.g., the first and second events in Nov 2007, as well as the event in Feb 2008, show improved timing. The model's ability to predict observed values was measured using the Nash Sutcliff efficiency (*E*), where values close to one indicate a perfect model. For our simulations in the *Rietholzbach* catchment, we found an improvement with the incorporation of the ASAR information where $E_{ASAR}=0.74$ and $E_{No\ ASAR}=0.70$.

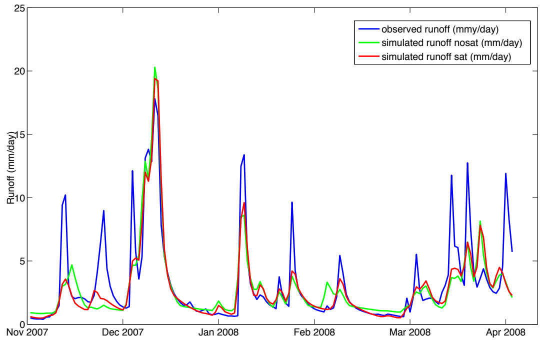

Figure 4: *Observed* versus *simulated* runoff (mm/day) without incorporation of water content derived from the wet snow maps (*no ASAR*, green)

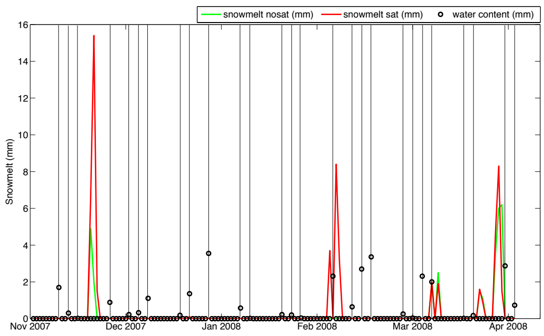

Figure 5: Simulated snowmelt with (red) and without (green) incorporation of water content derived from ASAR for the snow accumulation and melt season 2007-2008 in the *Rietholzbach* catchment. Black circles indicate the water content derived from the wet snow maps and correspond to the ASAR acquisitions

Figure 5 shows the simulated snowmelt together with the water content derived incorporating the ASAR observations. Slight differences are visible in the snowmelt between the two simulations and 27 water content updates for the 2007-8 snow season, corresponding to the 27 acquisitions for this period. Once the water content is updated in the model, it can remain in the snowpack for a period of time and even refreeze, so that the water content updates may not be directly seen in the snowmelt. Nevertheless, the additional information derived from the wet snow maps leads to slight improvements in the timing of the higher flow events as seen in the runoff. This is an important improvement for catchments not dominated by a spring snowmelt period, but have snow accumulation (as well as rainfall) and snow melt throughout the snow season. This preliminary study shows promising results for this type of catchment and a follow-on study will look at the larger *Thur* catchment in Switzerland. We will incorporate the water content into the HBV calibration phase in order to make improvements to the snow routine in the model.

4 OPERATIONAL INTEGRATION AT NATIONAL LEVEL

The Swiss Institute for Snow and Avalanche Research SLF runs an operational snow hydrological service (*OSHD*) that provides a range of different snow products for the Swiss federal flood forecasting. Apart from snow data from monitoring networks, and meteorological data from numerical weather forecast models, remote sensing data provide valuable information about the spatial extent of snow. Optical remote sensing data is however often unavailable due to cloud cover. The Envisat ASAR imagery captured for this project for the first time provided remote sensing data that was both weather-independent and at a sufficient spatial and temporal resolution to be used for operational snow water resources monitoring.

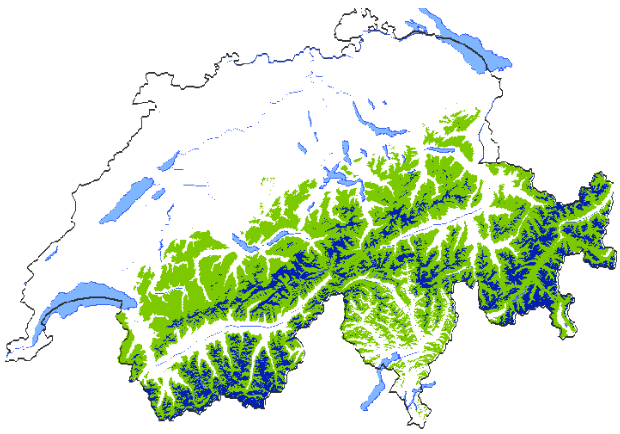

Figure 6: Snow classification based on ASAR scene from April 2nd, 2012. White denotes areas with no snow, green wet snow, blue dry snow.

Moreover, the ASAR imagery provided additional information on the superficial wetness of snow. Although melt water release depends on the liquid water content of the entire snowpack, any spatially explicit information on the hydrological state of the snowpack is a welcome addition. In the Alps it can take 2 to 3 weeks between the snow becoming wet at the surface and the first release of melt water. Thus, an extra effort is required to bridge the gap between snow wetness as seen by ASAR and snow wetness that is relevant to snowmelt runoff.

4.1 Data Integration

We have developed tools to integrate the ASAR imagery provided by RSL into the model platform run by OSHD. Apart from data management issues, this included the automation of a snow classification scheme based on jointly developed methods [17]. A resulting snow classification map is shown in Figure 6. The snow classification for this date compares well with snow model results for a congruent snow classification as seen in Figure 7. In particular, the spatial extent of wet snow cover is in good agreement between the ASAR-based classification (blue shading in Figure 6) and the results from the OSHD snow melt model (white shading in Figure 7). This comparison demonstrates that operational access to ASAR imagery can provide a valuable backup to independently check the plausibility of model results.

To support short-term hydrological forecasts, it is necessary to identify elevation bands that currently contribute to snow melt runoff. These data are typically drawn from the output of our snowmelt model. However, a direct interface between ASAR imagery and OSHD model evaluation tools has been created allowing assessment of the remote sensing data in a similar manner. An aggregation of ASAR-based snow classes within specific elevation bands and slope categories is exemplarily shown in Figure 8. The occurrence of wet snow varies with aspect, indicating higher percentages in southwest-facing slopes relative to northeast-facing slopes above the snow line for respective heights. These results agree well with corresponding evaluations from the output of the OSHD snowmelt model (data not shown).

Figure 7: Snow classification based on OSHD snow model results from April 4th, 2012. Green denotes areas with no snow, red wet snow, white dry snow.

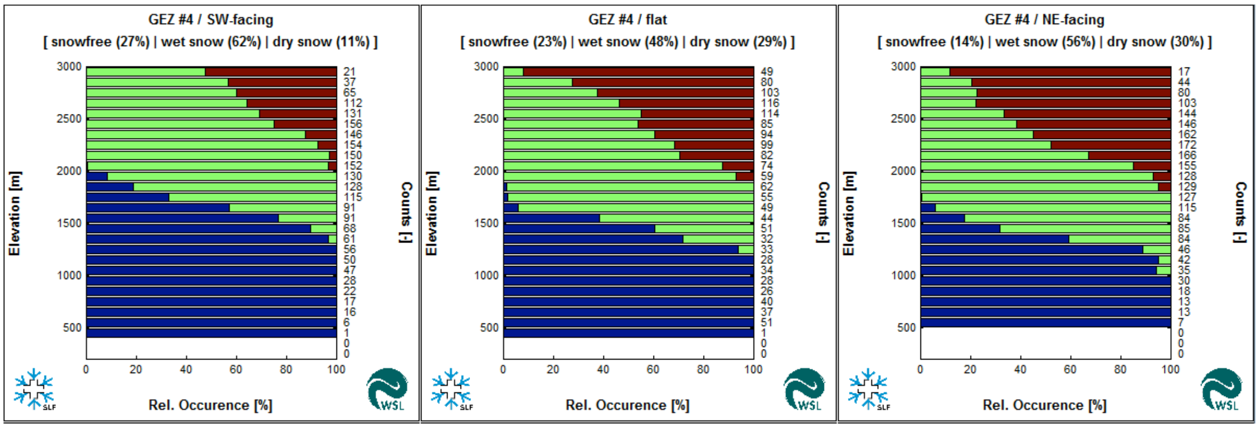

Figure 8: Regional breakdown of snow classification into elevation bands for flat, SW-facing, NE-facing areas. The evaluation of the catchment of the Alpine Rhine is based on the classification data shown in Figure 6. Blue denotes areas with no snow, green wet snow, red dry snow.

4.2 ASAR to Snow Hydrology in Near Real Time

RSL and SLF were together able to set up near-real-time (NRT) access to processed ASAR products and integrate them into the OSHD model and analysis platform. Due to the unexpected and premature termination of the project due to loss of contact with the satellite, it was not possible to test the practical applicability of the incoming images over an entire snowmelt season. We continue to investigate appropriate methodologies to bridge the gap between snow wetness as seen by ASAR and snow wetness that is relevant to snowmelt runoff. Given regular wide-swath observations of a few melting seasons, a direct dynamic assimilation of SAR data into the OSHD snowmelt model might become realistic.

5 CONCLUSIONS & OUTLOOK

Although the premature loss of contact with Envisat in April 2012 cut short the planned project, the exercise was educational, alerting us to possible stumbling blocks to near-real-time integration.

The following lessons were learned:

- Poor state vector quality (e.g. in extraordinary cases, when *predicted quality* state vectors generated 3 days before the acquisition are used during product generation) can delay provision of higher level products that depend on accurate geolocation
- No other sensor was able to substitute for the loss of the dense ASAR time series after the demise of ENVISAT. Ordering Radarsat-2 ScanSAR narrow data was too expensive and uncertain due to conflicts in central Europe.

These experiences will be valuable when preparing for the high temporal density expected from the Sentinel-1 mission's interferometric wideswath (IW) mode acquisitions over land [24]. "S1A", the first of two Sentinel-1 satellites, is due to be launched in 2014, with a 12-day orbital repeat cycle, acquiring mainly in the new IW TOPSAR ScanSAR mode [5] (250km swath width). The spatial and temporal resolutions it provides will enable further improvements to wet-snow mapping in the Swiss Alps. Once the second satellite "S1B" is launched, a 6-day exact repeat will be possible, and even finer temporal resolution given the type of integration of multi-track observations that we have demonstrated.

It should be understood that enabling analysis of wet snow extent with temporal resolutions *higher than the exact repeat interval* (12 days for one satellite, 6 days given two) will require integration of multi-track acquisitions, whereby radiometric terrain correction will play a key role. Integration of backscatter estimates from diverse geometries (e.g. into composite backscatter products [20]) will be necessary to maintain consistently high mapping quality, even in the presence of severe foreshortening and layover phenomena. Application of these techniques will have the added benefit of easing the integration of data from additional sensors (e.g. the three planned C-band Canadian Radarsat Constellation sensors, or 200km ScanSAR X-band data from the German TSX/TDX and Spanish PAZ) satellites.

6 ACKNOWLEDGMENTS

The Envisat ASAR data acquisitions from 2012 were kindly provided by ESA within the frame of EOPI project 10331. The Swiss DHM25 height model from *swisstopo* was used for all geocoding and radiometric terrain corrections applied to the ASAR data.

7 REFERENCES

[1] Andreadis, K.M. & Lettenmaier, D.P. (2006). Assimilating remotely sensed snow observations into a macroscale hydrology model, *Advances in Water Resources*, 29, pp. 872–886. doi: 10.1016/j.advwatres.2005.0

[2] Atwood, D.K., Small, D. & Gens, R. (2012). Improving PolSAR Land Cover Classification With Radiometric Correction of the Coherency Matrix. *Journal of Selected Topics in Applied Earth Observations and Remote Sensing*, 5(3), pp. 848–856. doi: 10.1109/JSTARS.2012.2186791

[3] Baghdadi, N., Gauthier, Y. & Bernier, M. (1997). Capability of Multitemporal ERS-1 SAR Data for Wet-Snow Mapping. *Remote Sensing of Environment*, 60(2), pp. 174–186. doi: 10.1016/S0034-4257(96)00180-0

[4] Bergström, S. (1992). The HBV Model: Its Structure and Applications, Swedish Meteorological and Hydrological Institute (SMHI), *Hydrology*, Norrköping, 35 p.

[5] De Zan, F. & Monti Guarnieri, A.M. (2006). TOPSAR: Terrain Observation by Progressive Scans. *Trans. on Geoscience and Remote Sensing*, 44(9), pp. 2352–2360. doi: 10.1109/TGRS.2006.873853

[6] Guneriussen, T., Johnsen, H. & Sand, K. (1996). DEM corrected ERS-1 SAR data for snow monitoring. *International Journal of Remote Sensing*, 17(1), pp. 181-195. doi: 10.1080/01431169608948994

[7] Haefner, H., Small D., Biegger S., Hoffman H., Nüesch, D. (2001). Small-Scale Monitoring of Wet Snowcover with Radarsat-ScanSAR Data. *EARSeL Workshop Special Interest Group Land Ice and Snow (LISSIG) on Remote Sensing of Snow and Glaciers*, Dresden, Germany, pp. 339–347. Available at: http://www.eproceedings.org/static/vol01_1/01_1_haefner1.pdf

[8] Koskinen, J.T., Pulliainen, J.T. & Hallikainen, M.T. (1997). The use of ERS-1 SAR data in snow melt monitoring. *Trans. on Geoscience and Remote Sensing*, 35(3), pp. 601–610. doi: 10.1109/36.581975

[9] Luojus, K.P., Pulliainen J., Metsamaki S., Hallikainen M. (2007). Snow-Covered Area Estimation Using Satellite Radar Wide-Swath Images. *Trans. on Geoscience and Remote Sensing*, 45(4), pp. 978–989. doi: 10.1109/TGRS.2006.888864

[10] Luojus, K.P., Pulliainen J., Metsamaki S., Hallikainen M. (2009). Enhanced SAR-Based Snow-Covered Area Estimation Method for Boreal Forest Zone. *Trans. on Geoscience and Remote Sensing*, 47(3), pp. 922–935. doi: 10.1109/TGRS.2008.2006047

[11] Malnes, E. & Guneriussen, T. (2002). Mapping of snow covered area with Radarsat in Norway. In *Proc. IGARSS*, pp. 683-685. doi: 10.1109/IGARSS.2002.1025145

[12] Miranda, N., Rosich B., Meadows P., et al. (2013). The Envisat ASAR Mission: A Look Back at 10 Years of Operation, Proc. *ESA Living Planet Symposium*, Edinburgh, Scotland.

[13] Nagler T. & Rott H. (2000). Retrieval of wet snow by means of multitemporal SAR data, *Trans. on Geoscience and Remote Sensing*, 38(2), pp. 754-765. doi: 10.1109/36.842004

[14] Nolin, A.W. (2010). Recent advances in remote sensing of seasonal snow. *Journal of Glaciology*, 56(200), pp. 1141-1150. doi: 10.3189/002214311796406077

[15] Parajka, J. & Blöschl G. (2008). The value of MODIS snow cover data in validating and calibrating conceptual hydrologic models, *Journal of Hydrology*, 258, pp. 240-258. doi: 10.1016/j.jhydrol.2008.06.006

[16] Piesbergen, J., Holecz, F. & Haefner, H. (1995). Snow cover monitoring using multitemporal ERS-1 SAR data. Proc. *IGARSS,* Florence, Italy, pp. 1750–1752. doi: 10.1109/IGARSS.1995.524015

[17] Schaub R. (2011). Validation of wet snow maps from Envisat/ASAR-Data, *M.Sc. Thesis*, Dept. of Geography, University of Zurich, Switzerland.

[18] Schubert, A., Jehle, M., Small, D. & Meier, E. (2012). Mitigation of atmospheric perturbations and solid Earth movements in a TerraSAR-X time-series. *Journal of Geodesy*, 86(4), pp. 257–270. doi: 10.1007/s00190-011-0515-6

[19] Seibert, J. and Vis, M. (2012). Teaching hydrological modeling with a user-friendly catchment-runoff-model software package. *Hydrology and Earth System Sciences*, 16, 3315–3325. doi: 10.5194/hess-16-3315-2012

[20] Small, D. (2012). SAR Backscatter Multitemporal Compositing via Local Resolution Weighting, Proc. *IGARSS*, Munich, Germany, pp. 4521–4524. doi: 10.1109/IGARSS.2012.6350465

[21] Small D., L. Zuberbühler, L., Schubert, A. & Meier E. (2011). Terrain-flattened gamma nought Radarsat-2 backscatter, *Canadian Journal of Remote Sensing*, 37(5), pp. 493–499, Oct. 2011. doi: 10.5589/m11-059

[22] Small D. (2011). Flattening Gamma: Radiometric Terrain Correction for SAR Imagery, *Trans. on Geoscience and Remote Sensing*, 49(8), pp. 3081–3093, Aug. 2011. doi: 10.1109/TGRS.2011.2120616

[23] Small D., Miranda N. & Meier, E. (2009). A revised radiometric normalisation standard for SAR, Proc. *IGARSS*, Cape Town, South Africa, pp. 566–569. doi: 10.1109/IGARSS.2009.5417439

[24] Torres, R., Snoeij P., Geudtner D., et al. (2012). GMES Sentinel-1 mission. *Remote Sensing of Environment*, 120, pp. 9–24. doi: 10.1016/j.rse.2011.05.028

[25] Valenti, L., Small D., Meier E. (2008). Snow cover monitoring using multitemporal ENVISAT/ASAR data. In S. Wunderle, ed. *EARSeL Workshop Special Interest Group Land Ice and Snow (LISSIG) on Remote Sensing of Snow and Glaciers*. Bern, Switzerland: European Association of Remote Sensing Laboratories, 8p. Available at: http://www.earsel.org/workshops/LISSIG2008/Valenti_Paper.pdf